Asymptotically Unbiased Instance-wise Regularized Partial AUC Optimization: Theory and Algorithm

Anonymous Author(s)
Affiliation
Address
email

Abstract

The Partial Area Under the ROC Curve (PAUC), typically including One-way Partial AUC (OPAUC) and Two-way Partial AUC (TPAUC), measures the average performance of a binary classifier within a specific false positive rate and/or true positive rate interval, which is a widely adopted measure when decision constraints must be considered. Consequently, PAUC optimization has naturally attracted increasing attention in the machine learning community within the last few years. Nonetheless, most of the existing methods could only optimize PAUC approximately, leading to inevitable biases that are not controllable. Fortunately, a recent work presents an unbiased formulation of the PAUC optimization problem via distributional robust optimization. However, it is based on the pair-wise formulation of AUC, which suffers from the limited scalability w.r.t. sample size and a slow convergence rate, especially for TPAUC. To address this issue, we present a simpler reformulation of the problem in an asymptotically unbiased and instance-wise manner. For both OPAUC and TPAUC, we come to a nonconvex strongly concave min-max regularized problem of instance-wise functions. On top of this, we employ an efficient solver which not only enjoys a linear per-iteration computational complexity w.r.t. the sample size but also improves the convergence rate for TPAUC optimization from $O(T^{-1/6})$ to $O(T^{-1/3})$ (T is the number of iteration). Furthermore, we find that the min-max reformulation also facilitates the theoretical analysis of generalization error as a byproduct. Compared with the existing results, we present new error bounds that are much easier to prove and could deal with hypotheses with real-valued outputs. Finally, extensive experiments on several benchmark datasets demonstrate the effectiveness of our method.

1 Introduction

AUC refers to the Area Under the Receiver Operating Characteristic (ROC) curve [1], where the ROC curve is obtained by plotting the True Positive Rate (TPR) against the False Positive Rate (FPR) of a given classifier for all possible thresholds. Since it is insensitive to the class distribution, AUC has become one of the standard metrics for long-tail, and imbalanced datasets [1, 22, 37]. Consequently, AUC optimization has attracted increasing attention in the machine learning community ever since the early 2000s [13, 5, 34, 17]. Over the last two decades, research on AUC optimization has evolved from the simplest linear models and decision trees [27, 10, 29, 40] to state-of-the-art deep learning architectures [21, 14, 36, 42, 41, 32]. With such remarkable success, one can now easily apply AUC optimization to deal with various real-world problems ranging from financial fraud detection[16, 4, 23], spam email detection [24], to medical diagnosis [24, 37, 36, 42], etc.

However, in such long-tailed applications, we are often interested in a specific region in the ROC curve where its area is called Partial AUC (PAUC). As illustrated in Fig.1, there are two types of PAUC.

Submitted to 36th Conference on Neural Information Processing Systems (NeurIPS 2022). Do not distribute.

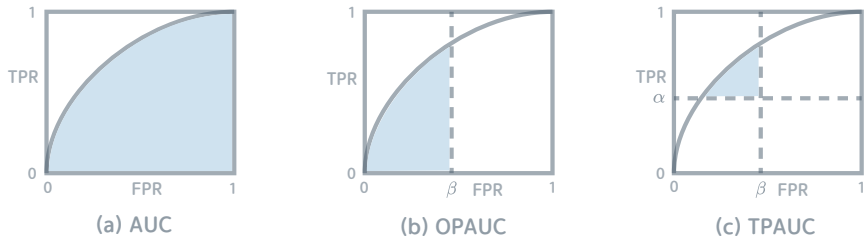

Figure 1: The comparison among different AUC variants. (a) The area under the ROC curve (AUC). (b) The one-way partial AUC (OPAUC). (c) The two-way partial AUC (TPAUC).

Table 1: Comparison with existing partial AUC algorithms. The convergence rate represents the number of iterations after which an algorithm can find an ϵ-stationary point, where ϵ is the precision tolerance. $\triangle$ implies a natural result of non-convex SGD. n_+(n_- resp.) is the number of positive (negative resp.) instances. $\kappa \to \infty$ implies that our method is unbiased when the κ goes to infinity for r_κ (see Eq.(15))

	DROE [43]	DROS [43]	DCA [39]	TPAUC [38]	Ours
Convergence Rate (OPAUC)	$O(\epsilon^{-4})$	$O(\epsilon^{-4})$	$O(\epsilon^{-6})$	$O(\epsilon^{-2})^{\triangle}$	$O(\epsilon^{-3})$
Convergence Rate (TPAUC)	$O(\epsilon^{-6})$	$O(\epsilon^{-4})$	-	$O(\epsilon^{-2})^{\triangle}$	$O(\epsilon^{-3})$
OPAUC&TPAUC	$\surd$	$\surd$	$\times$	$\surd$	$\surd$
Unbiased	$\surd$	$\times$	$\times$	$\times$	$\kappa \to \infty$
Per-Iteration Time Complexity	$O(n_+n_-)$	$O(n_+n_-)$	$O(n_+n_-)$	$O(n_+n_-)$	$O(n_+ + n_-)$

Here, One-way Partial AUC (OPAUC) measures the area within an FPR interval ($0 \leq \text{FPR} \leq \beta$); while Two-way Partial AUC (TPAUC) measures the area with $\text{FPR} \leq \beta$, $\text{TPR} \geq \alpha$. Unlike the full AUC, optimizing PAUC requires selecting top-ranked or/and bottom-ranked instances, leading to a hard combinatorial optimization problem. Many efforts have been made to solve the problem [6, 24, 25, 20, 38]. However, the majority of them rely on full-batch optimization and the approximation of the top (bottom)-k ranking process, which suffers from immeasurable biases and undesirable efficiency. Most recently, researchers have started to explore mini-batch PAUC optimization for deep learning models. [38] proposed a novel end-to-end optimization framework for PAUC. This formulation has a fast convergence rate with the help of a stochastic optimization algorithm, but the estimation of PAUC is still biased. Later, [43] proposed a Distributional Robust Optimization (DRO) framework for PAUC optimization, where the bias can be eliminated by a clever reformulation and the compositional SGD algorithms [28]. However, they adopt the pair-wise loss function which has limited scalability w.r.t. sample size and $O(\epsilon^{-4})$/$O(\epsilon^{-6})$ time complexity to reach the ϵ-stationary point for OPAUC/TPAUC. Considering the efficiency bottleneck comes from the pair-wise formulation, we will explore the following question in this paper:

Can we design a simpler, asymptotically unbiased and instance-wise formulation to optimize OPAUC and TPAUC in an efficient way?

To answer this question, we propose an efficient and asymptotically unbiased optimization algorithm for regularized PAUC maximization with a faster convergence guarantee. The comparison with previous results are listed in Tab.1. We consider both OPAUC and TPAUC maximization, where for OPAUC, we focus on maximizing PAUC in the region: $\text{FPR} \leq \beta$ and for TPAUC we focus on the region: $\text{FPR} \leq \beta$ and $\text{TPR} \geq \alpha$. We summarize our contributions below.

- With a proper regularization, we propose a nonconvex strongly concave min-max instance-wise formulation for OPAUC and TPAUC maximization. On top of our proposed formulation, we employ an efficient stochastic min-max algorithm that finds a ϵ-stationary point within $O(\epsilon^{-3})$ iterations.
- We conduct a generalization analysis of our proposed methods. Our instance-wise reformulation can overcome the interdependent issue of the original pair-wise generalization analysis. The proof is much easier than the existing results. Moreover, compared with [25, 38], it can be applied to any real-valued hypothesis functions other than the hard-threshold functions.

- We conduct extensive experiments on multiple imbalanced image classification tasks. The experimental results speak to the effectiveness of our proposed methods.

2 Preliminaries

Notations. In this section, we give some definitions and preliminaries about OPAUC and TPAUC. Let $\mathcal{X} \subseteq \mathbb{R}^d$ be the input space, $\mathcal{Y} = \{0, 1\}$ be the label space. We denote $\mathcal{D}_\mathcal{P}$ and $\mathcal{D}_\mathcal{N}$ as positive and negative instance distribution, respectively. Let $S = \{\boldsymbol{z}_i = (\boldsymbol{x}_i, y_i)\}_{i=1}^n$ be a set of training data drawn from distribution $\mathcal{D}_\mathcal{Z}$, where n is the number of samples. Let $\mathcal{P}$ ($\mathcal{N}$ resp.) be a set of positive (negative resp.) instances in the dataset. **In this paper we only focus on the scoring functions** $f : \mathcal{X} \mapsto [0, 1]$. The output range can be simply implemented by any deep neural network with sigmoid outputs.

Standard AUC. The standard AUC calculates the entire area under the ROC curve. For mathematical convenience, our arguments start with the pair-wise reformulation of AUC. Specifically, as shown in [1], AUC measures the probability of a positive instance having a higher score than a negative instance:

$$\mathrm{AUC}(f) = \Pr_{\boldsymbol{x}\sim\mathcal{D}_\mathcal{P}, \boldsymbol{x}'\sim\mathcal{D}_\mathcal{N}} \left[f(\boldsymbol{x}) > f(\boldsymbol{x}') \right]. \tag{1}$$

OPAUC. As mentioned in the introduction, instead of considering the entire region of ROC, we focus on two forms of PAUC, namely TPAUC and OPAUC. According to [6], OPAUC is equivalent to the probability of a positive instance $\boldsymbol{x}$ being scored higher than a negative instance $\boldsymbol{x}'$ within the specific range $f(\boldsymbol{x}') \in [\eta_\beta(f), 1]$ *s.t.* $\Pr_{\boldsymbol{x}'\sim\mathcal{D}_\mathcal{N}} [f(\boldsymbol{x}') \geq \eta_\beta] = \beta$:

$$\mathrm{OPAUC}(f) = \Pr_{\boldsymbol{x}\sim\mathcal{D}_\mathcal{P}, \boldsymbol{x}'\sim\mathcal{D}_\mathcal{N}} \left[f(\boldsymbol{x}) > f(\boldsymbol{x}'), f(\boldsymbol{x}') \geq \eta_\beta(f) \right]. \tag{2}$$

Practically, we do not know the exact data distributions $\mathcal{D}_\mathcal{P}$, $\mathcal{D}_\mathcal{N}$ to calculate (2). Therefore, we turn to the empirical estimations of (2). Given a finite dataset S with n instances, let n_+, n_- be the numbers of positive/negative instances, respectively. For the OPAUC, its empirical estimation could be expressed as [24]:

$$\hat{\mathrm{AUC}}_\beta(f, S) = 1 - \sum_{i=1}^{n_+} \sum_{j=1}^{n_-^\beta} \frac{\ell_{0,1}(f(\boldsymbol{x}_i) - f(\boldsymbol{x}'_{[j]}))}{n_+ n_-^\beta}, \tag{3}$$

where $n_-^\beta = \lfloor n_- \cdot \beta \rfloor$; $\boldsymbol{x}'_{[j]}$ denotes the j-th largest score among negative samples; $\ell_{0,1}(t)$ is the $0-1$ loss, which returns 1 if $t < 0$ and 0 otherwise.

TPAUC. More recently, [35] argued that an efficient classifier should have low FPR and high TPR simultaneously. Therefore, we also study a more general variant called Two-way Partial AUC (TPAUC), where the restricted regions satisfy $\mathrm{TPR} \geq \alpha$ and $\mathrm{FPR} \leq \beta$. Similar to OPAUC, TPAUC measures the probability that a positive instance $\boldsymbol{x}$ ranks higher than a negative instance $\boldsymbol{x}'$ where $f(\boldsymbol{x}) \in [0, \eta_\alpha(f)]$, *s.t.* $\Pr_{\boldsymbol{x}\sim\mathcal{D}_\mathcal{P}} [f(\boldsymbol{x}) \leq \eta_\alpha] = \alpha$, $f(\boldsymbol{x}') \in [\eta_\beta(f), 1]$ *s.t.* $\Pr_{\boldsymbol{x}'\sim\mathcal{D}_\mathcal{N}} [f(\boldsymbol{x}') \geq \eta_\beta] = \beta$.

$$\mathrm{TPAUC}(f) = \Pr_{\boldsymbol{x}\sim\mathcal{D}_\mathcal{P}, \boldsymbol{x}'\sim\mathcal{D}_\mathcal{N}} \left[f(\boldsymbol{x}) > f(\boldsymbol{x}'), f(\boldsymbol{x}) \leq \eta_\alpha(f), f(\boldsymbol{x}') \geq \eta_\beta(f) \right]. \tag{4}$$

Similarly to OPAUC, for the TPAUC, we adopt its empirical estimation [35, 38]:

$$\hat{\mathrm{AUC}}_{\alpha,\beta}(f, S) = 1 - \sum_{i=1}^{n_+^\alpha} \sum_{j=1}^{n_-^\beta} \frac{\ell_{0,1}(f(\boldsymbol{x}_{[i]}) - f(\boldsymbol{x}'_{[j]}))}{n_+^\alpha n_-^\beta}, \tag{5}$$

where $n_+^\alpha = \lfloor n_+ \cdot \alpha \rfloor$, and $\boldsymbol{x}_{[i]}$ is i-th smallest score among all positive instances.

3 Problem Formulation

In this section, we introduce how to optimize OPAUC and TPAUC in an asymptotically unbiased instance-wise manner. Note that (3) and (5) are hard to optimize since it is complicated to determine the positive quantile $\eta_\alpha(f)$ and the negative quantile $\eta_\beta(f)$. So we can not obtain the bottom-ranked positive instances and top-ranked negative instances directly. In this section, we will elaborate on how to tackle these challenges.

3.1 Optimizing the OPAUC

According to Eq.(3), given a surrogate loss ℓ and the finite dataset S, maximizing OPAUC and $\hat{\mathrm{AUC}}_\beta(f, S)$ is equivalent to solving the following problems, respectively:

$$\min_f \mathcal{R}_\beta(f) = \mathbb{E}_{\boldsymbol{x}\sim\mathcal{D}_\mathcal{P}, \boldsymbol{x}'\sim\mathcal{D}_\mathcal{N}} \left[\mathbb{I}_{f(\boldsymbol{x}')\geq\eta_\beta(f)} \cdot \ell(f(\boldsymbol{x}) - f(\boldsymbol{x}'))\right], \tag{6}$$

$$\min_f \hat{\mathcal{R}}_\beta(f, S) = \sum_{i=1}^{n_+} \sum_{j=1}^{n_-^\beta} \frac{\ell(f(\boldsymbol{x}_i) - f(\boldsymbol{x}'_{[j]}))}{n_+ n_-^\beta}. \tag{7}$$

Step 1: Instance-wise Reformulation. Here, to simplify the reformulation, we will use the most popular squared loss $\ell(x) = (1-x)^2$. Under this setting, the following theorem shows an instance-wise reformulation of the OPAUC optimization problem (please see Appendix.E for the proof):

Theorem 1. *Assuming that $f(\boldsymbol{x}) \in [0,1]$, $\forall x \in \mathcal{X}$, $F_{op}(f, a, b, \gamma, t, \boldsymbol{z})$ is defined as:*

$$\begin{aligned} F_{op}(f, a, b, \gamma, t, \boldsymbol{z}) = &(f(\boldsymbol{x}) - a)^2 y + (f(\boldsymbol{x}) - b)^2 (1-y) \mathbb{I}_{f(\boldsymbol{x})\geq t} \\ &+ 2(1+\gamma) f(\boldsymbol{x})(1-y)\mathbb{I}_{f(\boldsymbol{x})\geq t} - 2(1+\gamma) f(\boldsymbol{x}) y - \gamma^2, \end{aligned} \tag{8}$$

we have the following conclusions:

*(a) (**Population Version**.) We have:*

$$\min_f \mathcal{R}_\beta(f) \Leftrightarrow \min_{f,(a,b)\in[0,1]^2} \max_{\gamma\in\Omega_\gamma} \mathop{\mathbb{E}}_{\boldsymbol{z}\sim\mathcal{D}_\mathcal{Z}} \left[F_{op}(f, a, b, \gamma, \eta_\beta(f), \boldsymbol{z})\right], \tag{9}$$

where $y = 1$ for positive instances, $y = 0$ for negative instances, Ω_γ is the constraint set of γ and $\eta_\beta(f) = \arg\min_{\eta_\beta\in\mathbb{R}} \hat{\mathbb{E}}_{\boldsymbol{x}'\sim\mathcal{D}_\mathcal{N}}[\mathbb{I}[f(\boldsymbol{x}') \geq \eta_\beta] = \beta]$.

*(b) (**Empirical Version**.) Moreover, given a training dataset S with sample size n, denote:*

$$\hat{\mathbb{E}}_{z\sim S}[F_{op}(f, a, b, \gamma, \hat{\eta}_\beta(f), \boldsymbol{z})] = \frac{1}{n}\sum_{i=1}^{n} F_{op}(f, a, b, \gamma, \hat{\eta}_\beta(f), \boldsymbol{z})$$

where $\hat{\eta}_\beta(f)$ is the empirical quantile of the negative instances in S. We have:

$$\min_f \hat{\mathcal{R}}_\beta(f, S) \Leftrightarrow \min_{f,(a,b)\in[0,1]^2} \max_{\gamma\in\Omega_\gamma} \hat{\mathop{\mathbb{E}}}_{\boldsymbol{z}\sim S} \left[F_{op}(f, a, b, \gamma, \hat{\eta}_\beta(f), \boldsymbol{z})\right], \tag{10}$$

Step 2: Differentiable Sample Selection. Thm.1 provides a support to convert the pair-wise loss into instance-wise loss for OPAUC. However, the min-max problem Eq.(10) is still difficult to solve due to the operation $\mathbb{I}_{f(\boldsymbol{x}'_j)\geq\eta_\beta(f)}$, which requires selecting top-ranked negative instances. To make the sample selection process differentiable, we adopt the following lemma.

Lemma 1. *(Lemma 1 [9]) $\sum_{i=1}^k x_{[i]}$ is a convex function of $(x_1, \cdots, x_n)$ where $x_{[i]}$ is the top-i element of a set $\{x_1, x_2, \cdots, x_n\}$. Furthermore, for $x_i, i = 1, \cdots, n$, we have $\sum_{i=1}^k x_{[i]} = \min_s\{ks + \sum_{i=1}^n [x_i - s]_+\}$, where $[a]_+ = \max\{0, a\}$.*

Lem.1 proposes an Average Top-k (ATk) loss which is the surrogate loss for top-k loss to eliminate the sorting problem. Optimizing the ATk loss is equivalent to selecting top-ranked instances. Actually, for $\mathcal{R}_\beta(f)$, we can just reformulate it as an Average Top-k (ATk) loss. Denote $\ell_-(\boldsymbol{x}') = (f(\boldsymbol{x}') - b)^2 + 2(1+\gamma)f(\boldsymbol{x}')$. In the proof of the next theorem, we will show that $\ell_-(\boldsymbol{x}')$ is an increasing function w.r.t. $f(\boldsymbol{x}')$, namely:

$$\sum_{j=1}^{n_-} \mathbb{I}_{f(\boldsymbol{x}'_j)\geq\eta_\beta(f)} \cdot \ell_-(\boldsymbol{x}'_j) = \sum_{j=1}^{n_-^\beta} \ell_-(\boldsymbol{x}')_{[j]}, \tag{11}$$

where $\ell_-(\boldsymbol{x}')_{[j]}$ is the j-th largest loss. And the similar result holds for $\hat{\mathcal{R}}_\beta(f, S)$. Then, we can reach to Thm.2 (please see Appendix.E for the proof):

Theorem 2. *Assuming that $f(\boldsymbol{x}) \in [0,1]$, for all $x \in \mathcal{X}$, we have the equivalent optimization for* OPAUC*:*

$$\min_{f,(a,b)\in[0,1]^2} \max_{\gamma\in\Omega_\gamma} \mathop{\mathbb{E}}_{\boldsymbol{z}\sim\mathcal{D}_{\mathcal{Z}}}[F_{op}(f,a,b,\gamma,\eta_\beta(f),\boldsymbol{z})] \Leftrightarrow \min_{f,(a,b)\in[0,1]^2} \max_{\gamma\in\Omega_\gamma} \min_{s'\in\Omega_{s'}} \mathop{\mathbb{E}}_{\boldsymbol{z}\sim\mathcal{D}_{\mathcal{Z}}}[G_{op}(f,a,b,\gamma,\boldsymbol{z},s')], \tag{12}$$

$$\min_{f,(a,b)\in[0,1]^2} \max_{\gamma\in\Omega_\gamma} \mathop{\hat{\mathbb{E}}}_{\boldsymbol{z}\sim S}[F_{op}(f,a,b,\gamma,\hat{\eta}_\beta(f),\boldsymbol{z})] \Leftrightarrow \min_{f,(a,b)\in[0,1]^2} \max_{\gamma\in\Omega_\gamma} \min_{s'\in\Omega_{s'}} \mathop{\hat{\mathbb{E}}}_{\boldsymbol{z}\sim S}[G_{op}(f,a,b,\gamma,\boldsymbol{z},s')], \tag{13}$$

where $\Omega_\gamma = [b-1,1]$, $\Omega_{s'} = [0,5]$ and

$$\begin{aligned} G_{op}(f,a,b,\gamma,\boldsymbol{z},s') = &[(f(\boldsymbol{x})-a)^2 - 2(1+\gamma)f(\boldsymbol{x})]y \\ &+ \left(\beta s' + \left[(f(\boldsymbol{x})-b)^2 + 2(1+\gamma)f(\boldsymbol{x}) - s'\right]_+\right)(1-y) - \gamma^2. \end{aligned} \tag{14}$$

Step 3: Asymptotically Unbiased Smoothing. Even with Thm.2, it is hard to optimize the min-max-min formulation in (13). A solution is to swap the order $\max_\gamma$ and $\min_{s'}$ to reformulate it as a min-max problem. The key obstacle to this idea is the non-smooth function $[\cdot]_+$. To avoid the $[\cdot]_+$, we apply the `softplus` function [12]:

$$r_\kappa(x) = \frac{\log\left(1+\exp(\kappa\cdot x)\right)}{\kappa}, \tag{15}$$

as a smooth surrogate. It is easy to show that $r_\kappa(x) \overset{\kappa\to\infty}{\to} [x]_+$. **Denote $G^\kappa_{op}(f,a,b,\gamma,\boldsymbol{z},s')$ the surrogate objective where the $[\cdot]_+$ in $G_{op}(f,a,b,\gamma,\boldsymbol{z},s')$ is replaced with $r_\kappa(\cdot)$.** We then proceed to solve the surrogate problem:

$$\min_{f,a,b} \max_{\gamma\in\Omega_\gamma} \min_{s'\in\Omega_{s'}} \mathop{\mathbb{E}}_{\boldsymbol{z}\sim\mathcal{D}_{\mathcal{Z}}}[G^\kappa_{op}(f,a,b,\gamma,\boldsymbol{z},s')], \quad \min_{f,a,b} \max_{\gamma\in\Omega_\gamma} \min_{s'\in\Omega_{s'}} \mathop{\hat{\mathbb{E}}}_{\boldsymbol{z}\sim S}[G^\kappa_{op}(f,a,b,\gamma,\boldsymbol{z},s')],$$

respectively for the population and empirical version.

Step 4: The Regularized Problem. It is easy to check that $r_\kappa(x)$ has a bounded second-order derivation. In this way, we can regard $G^\kappa_{op}(f,a,b,\gamma,\boldsymbol{z},\hat{\eta}_\beta(f),s')$ as a weakly-concave function [3] (please see Appendix.D for the definition) of γ. By employing an ℓ_2 regularization, we turn to a regularized form:

$$G^{\kappa,\omega}_{op}(f,a,b,\gamma,\boldsymbol{z},s') = G^\kappa_{op}(f,a,b,\gamma,\boldsymbol{z},s') - \omega\cdot\gamma^2,$$

With a sufficiently large ω, $G^{\kappa,\omega}_{op}(f,a,b,\gamma,\boldsymbol{z},s')$ is strongly-concave w.r.t. γ when all the other variables are fixed. We then reach a min-max problem in the final step.

Step 5: Min-Max Swapping. According to min-max theorem [3], if we replace $F^\kappa_{op}(f,a,b,\gamma,\boldsymbol{z},s')$ with $G^{\kappa,\omega}_{op}(f,a,b,\gamma,\boldsymbol{z},s')$, the surrogate optimization problem satisfies:

$$\min_{f,(a,b)\in[0,1]^2} \max_{\gamma\in\Omega_\gamma} \min_{s'\in\Omega_{s'}} \mathop{\mathbb{E}}_{\boldsymbol{z}\sim\mathcal{D}_{\mathcal{Z}}}[G^{\kappa,\omega}_{op}] \Leftrightarrow \min_{f,(a,b)\in[0,1]^2,s'\in\Omega_{s'}} \max_{\gamma\in\Omega_\gamma} \mathop{\mathbb{E}}_{\boldsymbol{z}\sim\mathcal{D}_{\mathcal{Z}}}[G^{\kappa,\omega}_{op}], \tag{16}$$

$$\min_{f,(a,b)\in[0,1]^2} \max_{\gamma\in\Omega_\gamma} \min_{s'\in\Omega_{s'}} \mathop{\hat{\mathbb{E}}}_{\boldsymbol{z}\sim S}[G^{\kappa,\omega}_{op}] \Leftrightarrow \min_{f,(a,b)\in[0,1]^2,s'\in\Omega_{s'}} \max_{\gamma\in\Omega_\gamma} \mathop{\hat{\mathbb{E}}}_{\boldsymbol{z}\sim S}[G^{\kappa,\omega}_{op}], \tag{17}$$

where $G^{\kappa,\omega}_{op} = G^{\kappa,\omega}_{op}(f,a,b,\gamma,\boldsymbol{z},s')$. In this sense, we come to a regularized non-convex strongly-concave problem. In Sec.4, we will employ an efficient solver to optimize the parameters.

3.2 Optimizing the TPAUC

According to (5), given a feasible surrogate loss ℓ and finite dataset S, maximizing TPAUC and $\hat{\mathrm{AUC}}_{\alpha,\beta}(f,S)$ is equivalent to solving the following problems, respectively:

$$\min_f \mathcal{R}_{\beta,\alpha}(f) = \mathbb{E}_{\boldsymbol{x}\sim\mathcal{D}_{\mathcal{P}},\boldsymbol{x}'\sim\mathcal{D}_{\mathcal{N}}}\left[\mathbb{I}_{f(\boldsymbol{x}')\geq\eta_\beta(f)}\cdot\mathbb{I}_{f(\boldsymbol{x})\leq\eta_\alpha(f)}\ell(f(\boldsymbol{x})-f(\boldsymbol{x}'))\right]. \tag{18}$$

$$\min_f \hat{\mathcal{R}}_{\beta,\alpha}(f,S) = \sum_{i=1}^{n_+^\alpha}\sum_{j=1}^{n_-^\beta} \frac{\ell(f(\boldsymbol{x}_{[i]})-f(\boldsymbol{x}'_{[j]}))}{n_+ n_-^\beta}. \tag{19}$$

Due to the limited space, we present the result directly, please refer to Appendix.B for more details.

Similar to OPAUC, we apply the function $r_\kappa(x)$, regularization $\omega\gamma^2$ and min-max theorem to solve the problem. In this sense, we can use

$$\min_{f,a,b,s,s'\in\Omega_s,\Omega_{s'}} \max_{\gamma\in\Omega_\gamma} \mathbb{E}_{\boldsymbol{z}\sim\mathcal{D}_{\mathcal{Z}}} \left[G_{tp}^{\kappa,\omega}\left(f,a,b,\gamma,\boldsymbol{z},s,s'\right)\right], \tag{20}$$

and

$$\min_{f,a,b,s,s'\in\Omega_s,\Omega_{s'}} \max_{\gamma\in\Omega_\gamma} \hat{\mathbb{E}}_{\boldsymbol{z}\sim S} \left[G_{tp}^{\kappa,\omega}\left(f,a,b,\gamma,\boldsymbol{z},s,s'\right)\right], \tag{21}$$

to minimize $\mathcal{R}_{\beta,\alpha}(f)$, and $\hat{\mathcal{R}}_{\beta,\alpha}(f)$, respectively. Here:

$$\begin{aligned} G_{tp}^{\kappa,\omega}(f,a,b,\gamma,\boldsymbol{z},s,s') = &\left(\alpha s + r_\kappa\left((f(\boldsymbol{x})-a)^2 - 2(1+\gamma)f(\boldsymbol{x}) - s\right)\right)y - (\omega+1)\gamma^2 \\ &+ \left(\beta s' + r_\kappa\left((f(\boldsymbol{x})-b)^2 + 2(1+\gamma)f(\boldsymbol{x}) - s'\right)\right)(1-y). \end{aligned} \tag{22}$$

4 Training Algorithm

According to the derivations in the previous sections, our goal is then to solve the resulting empirical min-max optimization problems in Eq.(17) and Eq.(21). It is easy to check that they are strongly-concave w.r.t γ whenever $\kappa \leq 2+\omega$, when $f(\boldsymbol{x}), a, b \in [0,1]$, $\gamma \in \Omega_\gamma$, $s, s' \in \Omega_s, \Omega_{s'}$. Therefore, we can adopt the nonconvex strongly concave min-max optimization algorithms to solve this problem [15]. In this section, following the work [15], we employ an accelerated stochastic gradient descent ascent (ASGDA) method to solve the min-max optimization problem. We denote $\boldsymbol{\theta} \in \mathbb{R}^d$ as the parameters of function f, $\boldsymbol{\tau} = \{\boldsymbol{\theta}, a, b, s, s'\} \in \Omega_\tau$ as the variables for the outer min-problem, where Ω_τ is the closed set. Algorithm 1 shows the framework of our ASGDA algorithm. There are two key steps. At `Line 5-6` of Algorithm 1, variables $\boldsymbol{\tau}_{t+1}$ and γ_{t+1} are updated in a momentum way. Moreover, the convex combination ensures that they are always feasible given that the initial solution is feasible. At `Line 9-10`, using the momentum-based variance reduced technique, we can estimate the stochastic first-order partial gradients $\boldsymbol{v}_t$ and w_t in a more stable manner.

Algorithm 1 ASGDA Stochastic Algorithm for Instance-wise Partial AUC Optimization

1: **Input**: Dataset $\mathcal{X}$, learning parameters $\{\nu, \lambda, k, m, c_1, c_2, T\}$
2: **Initialize:** Randomly select $\boldsymbol{\tau}_0 = \{\boldsymbol{\theta}_0, a_0, b_0, s_0, s_0'\}$ from $\Omega_{\boldsymbol{\tau}}$, $\boldsymbol{v}_0 = \mathbf{0}^d$, $w_0 = 0$.
Randomly select γ_0 from Ω_γ, $t = 0$,
3: **for** $t = 0, 1, \cdots, T$ **do**
4: Compute the learning rate $\eta_t = \frac{k}{(m+t)^{1/3}}$;
5: Update $\boldsymbol{\tau}_{t+1} = (1-\eta_t)\boldsymbol{\tau}_t + \eta_t \mathcal{P}_{\Omega_{\boldsymbol{\tau}}}(\boldsymbol{\tau}_t - \nu \boldsymbol{v}_t)$;
6: Update $\gamma_{t+1} = (1-\eta_t)\gamma_t + \eta_t \mathcal{P}_{\Omega_\gamma}(\gamma_t + \lambda w_t)$;
7: Compute $\rho_{t+1} = c_1\eta_t^2$ and $\xi_{t+1} = c_2\eta_t^2$;
8: Sampling mini-batch data $\mathcal{B}_{t+1}$ from dataset $\mathcal{X}$;
9: Update $\boldsymbol{v}_{t+1} = \nabla_{\boldsymbol{\tau}} G_{(\cdot)}(\boldsymbol{\tau}_{t+1}, \gamma_{t+1}; \mathcal{B}_{t+1}) + (1-\rho_{t+1})[\boldsymbol{v}_t - \nabla_{\boldsymbol{\tau}} G_{(\cdot)}(\boldsymbol{\tau}_t, \gamma_t, \mathcal{B}_{t+1})]$;
10: Update $w_{t+1} = \nabla_\gamma G_{(\cdot)}(\boldsymbol{\tau}_{t+1}, \gamma_{t+1}; \mathcal{B}_{t+1}) + (1-\xi_{t+1})[w_t - \nabla_\gamma G_{(\cdot)}(\boldsymbol{\tau}_t, \gamma_t, \mathcal{B}_{t+1})]$;
11: **end for**
12: **Return** $\boldsymbol{\theta}_{T+1}$

With the following smoothness assumption, we show the convergence rate in Thm.3.

Assumption 1. *$G_{(\cdot)}(\boldsymbol{\tau}, \gamma; \mathcal{B})$ has Lipschitz continuous gradients, i.e., there is a positive scalar L_G such that for any $\boldsymbol{\tau}, \boldsymbol{\tau}' \in \Omega_{\boldsymbol{\tau}}$, $\gamma, \gamma' \in \Omega_\gamma$,*

$$\|\nabla G_{(\cdot)}(\boldsymbol{\tau}, \gamma; \mathcal{B}) - \nabla G_{(\cdot)}(\boldsymbol{\tau}', \gamma'; \mathcal{B})\| \leq L_G(\|\boldsymbol{\tau} - \boldsymbol{\tau}'\| + \|\gamma - \gamma')\|). \tag{23}$$

Theorem 3. *(Theorem 9 [15]) Supposing that Asm.1 holds, let $\{\boldsymbol{\tau}_t, \gamma_t\}$ be a sequence generated by our method, if the learning rate satisfies:*

$$\begin{aligned} &c_1 \geq \frac{2}{3k^3} + \frac{9\tau^2}{4}, \qquad c_2 \geq \frac{2}{3k^3} + \frac{75L_G^2}{2} \\ &m \geq \max(2, k^3, (c_1 k)^3, (c_2 k)^3), \lambda \leq \min\left(\frac{1}{6L_G}, \frac{27b\mu}{16}\right) \\ &\nu \leq \min\left(\frac{\lambda\tau}{2L_G}\sqrt{\frac{2b}{8\lambda^2 + 75(L_G/\mu)^2 b}}, \frac{m^{1/3}}{2(L_G + \frac{L_G^2}{\mu})k}\right). \end{aligned} \tag{24}$$

Then we have:

$$\frac{1}{T}\sum_{t=1}^{T}\mathbb{E}\left[\left\|\frac{1}{\nu}(\boldsymbol{\tau}_t - \mathcal{P}_{\Omega_{\boldsymbol{\tau}}}(\boldsymbol{\tau}_t - \nu \boldsymbol{v}_t))\right\|\right] \leq \frac{2\sqrt{3M''}m^{1/6}}{T^{1/2}} + \frac{2\sqrt{3M''}}{T^{1/3}}, \tag{25}$$

where $\|\frac{1}{\nu}(\boldsymbol{\tau}_t - \mathcal{P}_{\Omega_{\boldsymbol{\tau}}}(\boldsymbol{\tau}_t - \nu\nabla F_{(\cdot)}(\boldsymbol{\tau}_t)))\|$ is the l_2-norm of gradient mapping metric for the outer problem [7, 11, 30] with $F_{(\cdot)}(\boldsymbol{\tau}_t) = \max_{\gamma\in\Omega_\gamma} G_{(\cdot)}(\boldsymbol{\tau}_t, \gamma)$. When $b = 1$, it is easy to verify that $k = O(1)$, $\lambda = O(\mu)$, $\nu^{-1} = O(L_G/\mu)$, $c_1 = O(1)$, $c_2 = O(L_G^2)$ and $m = O(L_G^6)$. Then we have $M'' = O(L_G^3/\mu^3)$. Thus, the algorithm has a convergence rate of $O(\frac{(L_G/\mu)^{3/2}}{T^{1/3}})$. By $\frac{(L_G/\mu)^{3/2}}{T^{1/3}} \leq \epsilon$, then the iteration number to achieve ϵ-first-order saddle point which satisfies: $T \geq (L_G/\mu)^{4.5}\epsilon^{-3}$.

5 Generalization Analysis

In this section, we theoretically analyze the generalization performance of our proposed estimators for OPAUC (please see the Appendix.F for the TPAUC). According to Thm.2 in Sec.3, we know that the generalization error of OPAUC with a surrogate loss ℓ can be measured as:

$$\mathcal{R}_\beta(f) \propto \min_{(a,b)\in[0,1]^2} \max_{\gamma\in\Omega_\gamma} \min_{s'\in\Omega_{s'}} \mathbb{E}_{\boldsymbol{z}\sim\mathcal{D}_{\mathcal{Z}}}[G_{op}(f, a, b, \gamma, \boldsymbol{z}, s')], \tag{26}$$

and

$$\hat{\mathcal{R}}_\beta(f) \propto \min_{(a,b)\in[0,1]^2} \max_{\gamma\in\Omega_\gamma} \min_{s'\in\Omega_{s'}} \hat{\mathbb{E}}_{\boldsymbol{z}\sim\mathcal{D}_{\mathcal{Z}}}[G_{op}(f, a, b, \gamma, \boldsymbol{z}, s')], \tag{27}$$

Following the ERM paradigm, to prove the uniform convergence result over a hypothesis class $\mathcal{F}$ of the scoring function f, we need to show that:

$$\sup_{f\in\mathcal{F}}\left[\mathcal{R}_\beta(f) - \hat{\mathcal{R}}_\beta(f)\right] \leq \epsilon.$$

According to the aforementioned discussion, we only need to prove that:

$$\begin{aligned} \sup_{f\in\mathcal{F}}\Big[&\min_{(a,b)\in[0,1]^2} \max_{\gamma\in\Omega_\gamma} \min_{s'\in\Omega_{s'}} \mathbb{E}_{\boldsymbol{z}\sim\mathcal{D}_{\mathcal{Z}}}[G_{op}(f, a, b, \gamma, \boldsymbol{z}, s')] \\ &- \min_{(a,b)\in[0,1]^2} \max_{\gamma\in\Omega_\gamma} \min_{s'\in\Omega_{s'}} \hat{\mathbb{E}}_{\boldsymbol{z}\sim\mathcal{D}_{\mathcal{Z}}}[G_{op}(f, a, b, \gamma, \boldsymbol{z}, s')]\Big] \leq \epsilon. \end{aligned}$$

To prove this, we need to define the measure of the complexity of the class $\mathcal{F}$. Here we adopt the Radermacher complexity $\Re$ as in [2] (please see Appendix.D for the definition). Specifically, we come to the following definition:

Definition 1. *The empirical Rademacher complexity of positive and negative instances with respect to S is defined as:*

$$\hat{\Re}_+(\mathcal{F}) = \mathbb{E}_{\boldsymbol{\sigma}}\left[\sup_{f\in\mathcal{F}} \frac{1}{n_+}\sum_{i=1}^{n_+}\sigma_i f(\boldsymbol{x}_i)\right], \tag{28}$$

$$\hat{\Re}_-(\mathcal{F}) = \mathbb{E}_{\boldsymbol{\sigma}}\left[\sup_{f\in\mathcal{F}} \frac{1}{n_-}\sum_{j=1}^{n_-}\sigma_i f(\boldsymbol{x}_j)\right] \tag{29}$$

where $(\sigma_1, \cdots, \sigma_m)$ are independent uniform random variables taking values in $\{-1, +1\}$.

Finally, we come to the generalization bound as follows:

Theorem 4. *For any $\delta > 0$, with probability at least $1-\delta$ over the draw of an i.i.d. sample set S of size m, for all $f \in \mathcal{F}$ we have:*

$$\min_{(a,b)\in[0,1]^2} \max_{\gamma\in\Omega_\gamma} \min_{s'\in\Omega_{s'}} \mathbb{E}_{\boldsymbol{z}\sim\mathcal{D}_{\mathcal{Z}}}[G_{op}(f,a,b,\gamma,\boldsymbol{z},s')] \leq \max_{\gamma\in\Omega_\gamma} \min_{s'\in\Omega_{s'}} \hat{\mathbb{E}}_{\boldsymbol{z}\sim S}[G_{op}(f,a,b,\gamma,\boldsymbol{z},s')] + O(\hat{\Re}_+(\mathcal{F}) + \hat{\Re}_-(\mathcal{F})) + O(n_+^{-1/2} + n_-^{-1/2})$$

Remark 1. *Although the results we obtain are similar to some previous studies. [38, 25], our generalization analysis is simpler and does not require complex error decomposition. Moreover, our results hold for all real-valued hypothesis class with outputs in $[0,1]$, while the previous results [38, 25] only hold for hard-threshold functions.*

6 Experiment

In this section, we conduct a series of experiments on different datasets for both OPAUC and TPAUC optimization. Due to space limitations, please refer to the Appendix.C for the details of implementation and competitors.

6.1 Setups

We adopt three imbalanced binary classification datasets: CIFAR-10-LT [8], CIFAR-100-LT [19] and Tiny-ImgaeNet-200-LT following the instructions in [38], where the binary datasets are constructed by selecting one super category as positive class and the other categories as negative class. Please see Appendix.C for more details. The evaluation metrics in experiments are $\hat{\text{AUC}}_\beta$ and $\hat{\text{AUC}}_{\alpha,\beta}$.

6.2 Overall Results

In Tab.2 and Tab.3, we record the performance on test sets of all the methods on three subsets of CIFAR-10-LT, CIFAR-100-LT, and Tiny-Imagent-200-LT. Each method is tuned independently for OPAUC and TPAUC metrics. From the results, we make the following remarks: (1) Our proposed methods outperform all the competitors on all the datasets in most cases, except for the CIFAR-100-LT Subset 3. Even for failure cases, our methods attain fairly competitive results compared with the competitors for OPAUC and TPAUC. (2) In addition, we can see that the normal AUC optimization method AUC-M has poor performance under PAUC metric. This demonstrates the necessity of developing the PAUC optimization algorithm. (3) Approximation methods like DROS, AUC-poly, and AUC-exp have lower performance than the unbiased algorithms. Above all, the empirical results suggest the effectiveness of our proposed method.

Table 2: OPAUC (FPR ≤ 0.3) on testing data of different imbalanced datasets. The highest and the second best results are highlighted in orange and blue, respectively.

	CIFAR-10-LT			CIFAR-100-LT			Tiny-Imagenet-LT		
Methods	Subset 1	Subset 2	Subset 3	Subset 1	Subset 2	Subset 3	Subset 1	Subset 2	Subset 3
DROE [43]	0.7659	0.9688	0.7651	0.9108	0.9875	0.8483	0.8157	0.9037	0.9066
DROS [43]	0.7548	0.9674	0.7542	0.9033	0.9860	0.8449	0.8180	0.9087	0.9095
AUC-poly [38]	0.7542	0.9672	0.7538	0.9027	0.9859	0.8441	0.8185	0.9084	0.9100
AUC-exp [38]	0.7347	0.9620	0.7457	0.8987	0.9850	0.8407	0.8127	0.9026	0.9049
CE	0.7417	0.9431	0.7428	0.8903	0.9695	0.8321	0.8023	0.8917	0.8878
MB [18]	0.7492	0.9648	0.7500	0.9003	0.9804	**0.8575**	0.8193	0.9072	0.9091
AUC-M [40]	0.7334	0.9609	0.7442	0.8996	0.9845	0.8403	0.8102	0.9011	0.9043
PAUCI	**0.7713**	**0.9718**	**0.7736**	**0.9199**	**0.9885**	0.8538	**0.8223**	**0.9124**	**0.9141**

6.3 Convergence Analysis

In the convergence experiments, for sake of fairness, we did not use warm-up. All algorithms use hyperparameters in the performance experiments. We show the plots of training convergence in Fig.2

Table 3: TPAUC ($\mathrm{TPR} \leq 0.5$, $\mathrm{FPR} \leq 0.5$) on testing data of different imbalanced datasets.

	CIFAR-10-LT			CIFAR-100-LT			Tiny-Imagenet-LT		
Methods	Subset 1	Subset 2	Subset 3	Subset 1	Subset 2	Subset 3	Subset 1	Subset 2	Subset 3
DROE [43]	0.7096	0.9593	0.7220	0.8714	0.9855	0.7485	0.7417	0.8681	0.8650
DROS [43]	0.6603	0.9456	0.6917	0.8617	0.9812	0.7419	0.7354	0.8666	0.8628
AUC-poly [38]	0.6804	0.9543	0.6974	0.8618	0.9835	0.7431	0.7349	0.8676	0.8627
AUC-exp [38]	0.6669	0.9493	0.6930	0.8613	0.9827	0.7447	0.7328	0.8672	0.8626
CE	0.6420	0.9353	0.6798	0.8467	0.9603	0.7311	0.7223	0.8517	0.8478
MB [18]	0.6437	0.9492	0.6913	0.8665	0.9677	**0.7583**	0.7348	0.8651	0.8624
AUC-M [40]	0.6520	0.9381	0.6821	0.8505	0.9822	0.7324	0.7361	0.8517	0.8598
PAUCI	**0.7112**	**0.9641**	**0.7406**	**0.8925**	**0.9874**	0.7574	**0.7727**	**0.8818**	**0.8794**

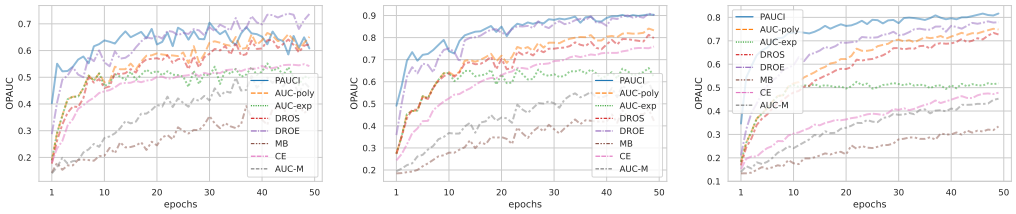

(a) CIFAR-10-LT-1 (b) CIFAR-10-LT-2 (c) CIFAR-10-LT-3

Figure 2: Convergence of OPAUC optimization.

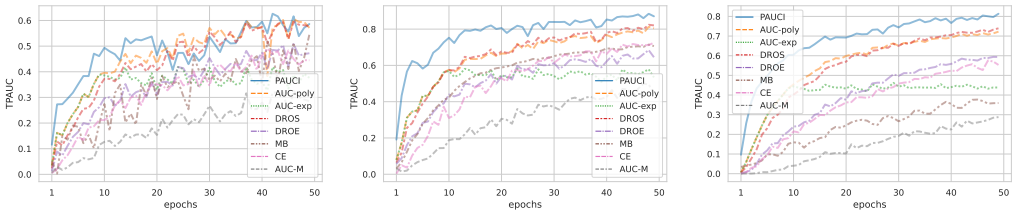

(a) CIFAR-10-LT-1 (b) CIFAR-10-LT-2 (c) CIFAR-10-LT-3

Figure 3: Convergence of TPAUC optimization.

and Fig.3 on CIFAR-10 for both OPAUC and TPAUC. Due to the space limitation, the other results could be found in Appendix.C. According to the figures, we can make the following observations: (1) Our algorithm and DROE converge faster than other methods for OPAUC. However, for TPAUC optimization, the DROE converges very slowly due to its complicated algorithm, while our method still shows the best convergence property in most cases. (2) It's notable that our algorithm converges to stabilize after twenty epochs in most cases. That means our method has better stability in practice.

7 Conclusion

In this paper, we focus on designing an efficient and asymptotically unbiased algorithm for PAUC. We propose a nonconvex strongly concave min-max instance-wise formulation for OPAUC and TPAUC. In this way, we incorporate the instances selection into the loss calculation to eliminate the score ranking challenge. For OPAUC and TPAUC, we employ an efficient stochastic min-max algorithm that ensures we can find a ϵ-first order saddle point after $O(\epsilon^{-3})$ iterations. Moreover, we present a theoretical analysis of the generalization error of our formulation. Our conclusion may contribute to future work about AUC generalization. Finally, empirical studies over a range of long-tailed benchmark datasets speak to the effectiveness of our proposed algorithm.

References

[1] J A, Hanley, B J, and McNeil. The meaning and use of the area under a receiver operating characteristic (roc) curve. *Radiology*, 1982.

[2] Peter L Bartlett and Shahar Mendelson. Rademacher and gaussian complexities: Risk bounds and structural results. *Journal of Machine Learning Research*, 3:463–482, 2002.

[3] Stephen Boyd, Stephen P Boyd, and Lieven Vandenberghe. *Convex optimization*. Cambridge university press, 2004.

[4] Dahee Choi and Kyungho Lee. Machine learning based approach to financial fraud detection process in mobile payment system. *IT Converg Pract*, 5(4):12–24, 2017.

[5] Corinna Cortes and Mehryar Mohri. AUC optimization vs. error rate minimization. In *Advances in Neural Information Processing Systems*, pages 313–320, 2003.

[6] Lori E. Dodd and Margaret S. Pepe. Partial auc estimation and regression. *Biometrics*, 59(3): 614–623, 2003.

[7] John C Dunn. On the convergence of projected gradient processes to singular critical points. *Journal of Optimization Theory and Applications*, 55(2):203–216, 1987.

[8] Jeremy Elson, John R. Douceur, Jon Howell, and Jared Saul. Asirra: a CAPTCHA that exploits interest-aligned manual image categorization. In *ACM Conference on Computer and Communications Security*, pages 366–374, 2007.

[9] Yanbo Fan, Siwei Lyu, Yiming Ying, and Baogang Hu. Learning with average top-k loss. *Advances in Neural Information Processing Systems*, 30:497–505, 2017.

[10] Yoav Freund, Raj Iyer, Robert E Schapire, and Yoram Singer. An efficient boosting algorithm for combining preferences. *Journal of Machine Learning Research*, 4:933–969, 2003.

[11] Saeed Ghadimi, Guanghui Lan, and Hongchao Zhang. Mini-batch stochastic approximation methods for nonconvex stochastic composite optimization. *Mathematical Programming*, 155 (1):267–305, 2016.

[12] Xavier Glorot, Antoine Bordes, and Yoshua Bengio. Deep sparse rectifier neural networks. In *International Conference on Artificial Intelligence and Statistics*, pages 315–323, 2011.

[13] Thore Graepel, Klaus Obermayer, et al. Large margin rank boundaries for ordinal regression. In *Advances in Large Margin Classifiers*, pages 115–132. 2000.

[14] Zhishuai Guo, Mingrui Liu, Zhuoning Yuan, Li Shen, Wei Liu, and Tianbao Yang. Communication-efficient distributed stochastic auc maximization with deep neural networks. In *International Conference on Machine Learning*, pages 3864–3874, 2020.

[15] Feihu Huang, Shangqian Gao, Jian Pei, and Heng Huang. Accelerated zeroth-order and first-order momentum methods from mini to minimax optimization. *Journal of Machine Learning Research*, 23(36):1–70, 2022.

[16] Mengda Huang, Yang Liu, Xiang Ao, Kuan Li, Jianfeng Chi, Jinghua Feng, Hao Yang, and Qing He. Auc-oriented graph neural network for fraud detection. In *ACM Web Conference*, pages 1311–1321, 2022.

[17] Thorsten Joachims. A support vector method for multivariate performance measures. In *International Conference on Machine Learning*, pages 377–384, 2005.

[18] Purushottam Kar, Harikrishna Narasimhan, and Prateek Jain. Online and stochastic gradient methods for non-decomposable loss functions. *Advances in Neural Information Processing Systems*, 27:694–702, 2014.

[19] Alex Krizhevsky, Geoffrey Hinton, et al. Learning multiple layers of features from tiny images. 2009.

[20] Abhishek Kumar, Harikrishna Narasimhan, and Andrew Cotter. Implicit rate-constrained optimization of non-decomposable objectives. In *International Conference on Machine Learning*, pages 5861–5871, 2021.

[21] Mingrui Liu, Zhuoning Yuan, Yiming Ying, and Tianbao Yang. Stochastic AUC maximization with deep neural networks. In *International Conference on Learning Representations*, 2020.

[22] Donna Katzman McClish. Analyzing a portion of the roc curve. *Medical Decision Making*, 9 (3):190–195, 1989.

[23] Aji Mubarek Mubalaike and Esref Adali. Deep learning approach for intelligent financial fraud detection system. In *nternational Conference on Computer Science and Engineering*, pages 598–603, 2018.

[24] Harikrishna Narasimhan and Shivani Agarwal. A structural svm based approach for optimizing partial auc. In *International Conference on Machine Learning*, pages 516–524, 2013.

[25] Harikrishna Narasimhan and Shivani Agarwal. Support vector algorithms for optimizing the partial area under the roc curve. *Neural Computation*, 29(7):1919–1963, 2017.

[26] Michael Natole, Yiming Ying, and Siwei Lyu. Stochastic proximal algorithms for auc maximization. In *International Conference on Machine Learning*, pages 3710–3719, 2018.

[27] Margaret Sullivan Pepe and Mary Lou Thompson. Combining diagnostic test results to increase accuracy. *Biostatistics*, 1(2):123–140, 2000.

[28] Qiqi, Youzhi Luo, Zhao Xu, Shuiwang Ji, and Tianbao Yang. Stochastic optimization of area under precision-recall curve for deep learning with provable convergence. *arXiv e-prints*, pages arXiv–2104, 2021.

[29] Alain Rakotomamonjy. Support vector machines and area under roc curve. *PSI-INSA de Rouen: Technical Report*, 2004.

[30] Meisam Razaviyayn, Tianjian Huang, Songtao Lu, Maher Nouiehed, Maziar Sanjabi, and Mingyi Hong. Nonconvex min-max optimization: Applications, challenges, and recent theoretical advances. *IEEE Signal Processing Magazine*, 37(5):55–66, 2020.

[31] Robert E Schapire and Yoav Freund. Foundations of machine learning. 2012.

[32] Guanghui Wang, Ming Yang, Lijun Zhang, and Tianbao Yang. Momentum accelerates the convergence of stochastic auprc maximization. In *International Conference on Artificial Intelligence and Statistics*, pages 3753–3771, 2022.

[33] Zhanfeng Wang and Yuan-Chin Ivan Chang. Marker selection via maximizing the partial area under the roc curve of linear risk scores. *Biostatistics*, 12(2):369–385, 2011.

[34] Lian Yan, Robert H Dodier, Michael Mozer, and Richard H Wolniewicz. Optimizing classifier performance via an approximation to the wilcoxon-mann-whitney statistic. In *International Conference on Machine Learning*, pages 848–855, 2003.

[35] Hanfang Yang, Kun Lu, Xiang Lyu, and Feifang Hu. Two-way partial auc and its properties. *Statistical Methods in Medical Research*, 28(1):184–195, 2019.

[36] Tianbao Yang. Deep auc maximization for medical image classification: Challenges and opportunities. *arXiv preprint arXiv:2111.02400*, 2021.

[37] Tianbao Yang and Yiming Ying. Auc maximization in the era of big data and ai: A survey. *arXiv preprint arXiv:2203.15046*, 2022.

[38] Zhiyong Yang, Qianqian Xu, Shilong Bao, Yuan He, Xiaochun Cao, and Qingming Huang. When all we need is a piece of the pie: A generic framework for optimizing two-way partial auc. In *International Conference on Machine Learning*, pages 11820–11829, 2021.

[39] Yao Yao, Qihang Lin, and Tianbao Yang. Large-scale optimization of partial auc in a range of false positive rates. *arXiv preprint arXiv:2203.01505*, 2022.

[40] Yiming Ying, Longyin Wen, and Siwei Lyu. Stochastic online auc maximization. *Advances in Neural Information Processing Systems*, 29:451–459, 2016.

[41] Zhuoning Yuan, Zhishuai Guo, Nitesh Chawla, and Tianbao Yang. Compositional training for end-to-end deep auc maximization. In *International Conference on Learning Representations*, 2021.

[42] Zhuoning Yuan, Yan Yan, Milan Sonka, and Tianbao Yang. Large-scale robust deep auc maximization: A new surrogate loss and empirical studies on medical image classification. In *IEEE/CVF International Conference on Computer Vision*, pages 3040–3049, 2021.

[43] Dixian Zhu, Gang Li, Bokun Wang, Xiaodong Wu, and Tianbao Yang. When auc meets dro: Optimizing partial auc for deep learning with non-convex convergence guarantee. *arXiv preprint arXiv:2203.00176*, 2022.

Checklist

1. For all authors...
   (a) Do the main claims made in the abstract and introduction accurately reflect the paper's contributions and scope? [Yes]
   (b) Did you describe the limitations of your work? [N/A]
   (c) Did you discuss any potential negative societal impacts of your work? [No] We have not discovered any negative societal impacts in our study.
   (d) Have you read the ethics review guidelines and ensured that your paper conforms to them? [Yes]
2. If you are including theoretical results...
   (a) Did you state the full set of assumptions of all theoretical results? [Yes]
   (b) Did you include complete proofs of all theoretical results? [Yes]
3. If you ran experiments...
   (a) Did you include the code, data, and instructions needed to reproduce the main experimental results (either in the supplemental material or as a URL)? [Yes]
   (b) Did you specify all the training details (e.g., data splits, hyperparameters, how they were chosen)? [Yes]
   (c) Did you report error bars (e.g., with respect to the random seed after running experiments multiple times)? [No] Our experiments are very time consuming.
   (d) Did you include the total amount of compute and the type of resources used (e.g., type of GPUs, internal cluster, or cloud provider)? [Yes]
4. If you are using existing assets (e.g., code, data, models) or curating/releasing new assets...
   (a) If your work uses existing assets, did you cite the creators? [Yes]
   (b) Did you mention the license of the assets? [Yes]
   (c) Did you include any new assets either in the supplemental material or as a URL? [Yes]
   (d) Did you discuss whether and how consent was obtained from people whose data you're using/curating? [No] Because we use the open source software and data.
   (e) Did you discuss whether the data you are using/curating contains personally identifiable information or offensive content? [N/A]
5. If you used crowdsourcing or conducted research with human subjects...
   (a) Did you include the full text of instructions given to participants and screenshots, if applicable? [N/A]
   (b) Did you describe any potential participant risks, with links to Institutional Review Board (IRB) approvals, if applicable? [N/A]
   (c) Did you include the estimated hourly wage paid to participants and the total amount spent on participant compensation? [N/A]